



# Transient hydrothermal corrugations within mineralized ultramafic laterites

Laurent Guillou-Frottier, Anicet Beauvais, Laurent Bailly, Robert Wyns,  
Thierry Augé, Anne-Sophie Audion

## ► To cite this version:

Laurent Guillou-Frottier, Anicet Beauvais, Laurent Bailly, Robert Wyns, Thierry Augé, et al.. Transient hydrothermal corrugations within mineralized ultramafic laterites. SGA 2015: Ressources minérales dans un monde durable, SGA (Society for Geology Applied to Mineral Deposits), Aug 2015, Nancy, France. hal-01157947

**HAL Id: hal-01157947**

**<https://brgm.hal.science/hal-01157947>**

Submitted on 29 May 2015

**HAL** is a multi-disciplinary open access archive for the deposit and dissemination of scientific research documents, whether they are published or not. The documents may come from teaching and research institutions in France or abroad, or from public or private research centers.

L'archive ouverte pluridisciplinaire **HAL**, est destinée au dépôt et à la diffusion de documents scientifiques de niveau recherche, publiés ou non, émanant des établissements d'enseignement et de recherche français ou étrangers, des laboratoires publics ou privés.



Distributed under a Creative Commons Attribution - NonCommercial - NoDerivatives 4.0  
International License

# Transient hydrothermal corrugations within mineralized ultramafic laterites

L. Guillou-Frottier<sup>1</sup>, A. Beauvais<sup>2</sup>, L. Bailly<sup>1</sup>, R. Wyns<sup>1</sup>, T. Augé<sup>1</sup> and A-S. Audion<sup>1,3</sup>

1: BRGM, ISTO, UMR 7327, Georesources Division, 3 av. C. Guillemin, BP 36009, 45060 Orléans Cedex 2, France

2 : Aix-Marseille University, IRD, CNRS, CEREGE UM 34, BP 80, 13545 Aix-en-Provence, Cedex 4, France

3: Now at Variscan Mines, 16 Rue Leonard de Vinci, 45100 Orléans, France

**Abstract.** Mineralization processes in ultramafic laterites are partly controlled by fluid flow regimes in these porous and permeable systems. During weathering of ultramafic rocks, exothermic chemical reactions, such as hydration of olivine, may generate shallow subsurface (< 200 m) temperatures of several tens of °C. The reaction-induced fracturing leads to further reactions and increases the permeability. For more than 20 Myr, the peridotite massifs of New Caledonia have undergone intense weathering, and the observable undulations along the weathering front, attest to a corrugated bedrock topography. Combined together, the excess heat (up to 70-90°C) and high permeability ( $10^{-14}$  to  $9 \times 10^{-13}$  m<sup>2</sup>) might have potentially triggered hydrothermal convection, as confirmed by Rayleigh number estimates. This was numerically modeled by accounting for temperature-dependent fluid properties, and for time-dependent and spatially varying parameters simulating the deepening of the weathering front. Modeling the transient evolution of the thermal and flow velocity fields over 10 Myr reveals that hydrothermal convection can develop in the New Caledonian laterites, even on sloped surfaces where topography-driven flow prevails. Convective cells develop above the weathering front, and the models reveal two-dimensional corrugations below which weathering is no longer efficient.

**Keywords:** hydrothermal convection; laterites; mineralization; ultramafic; New Caledonia

## 1 Introduction

Understanding the fluid flow regime within ultramafic laterites is crucial to establishing the links between weathering and mineralization. As previously described in New Caledonia (NC), weathering of olivine and pyroxene results in leaching of Si and Mg, which can however re-precipitate in Si-Mg gels, amorphous silica, smectite and/or magnesite along open fractures at the bottom of the saprolite. Newly formed minerals such as smectite (Trescases, 1975), “garnierite” (the local name for nickel-bearing phyllosilicates), and Fe-Mn oxyhydroxides in the lower saprolite host Ni, Co and Mn.

However, some puzzling questions and observations remain, such as the inhomogeneity of nickel grade within the mineralized laterites, and the undulated lithological interfaces, including the weathering front itself, which shows three-dimensional corrugations (or “egg-box topography”). This study is mainly focused on the investigation of the second point, which in turn should bring new insights to the understanding of mineralizing processes.

After describing the geological data and physico-chemical processes within lateritic mantles, we

quantitatively investigate the impact of exothermic reactions along the weathering front where permeability and heat production are enhanced. The role of surface topographic slope on groundwater flow regimes is also investigated. Realistic petrophysical properties are taken into account, and the deepening of the weathering front is simulated. The unknown parameters are adjusted to retrieve field data and observations. One challenging goal is to document the physical processes controlling subsurface fluid flow in a dynamic system where the bottom boundary deepens with time, thus involving a time-dependent geometry

## 2 Reaction-induced fracturing and heating

Aqueous weathering of rocks involves numerous physical and chemical processes that result in important changes in rock compositions, properties and morphologies (e.g. Jamtveit and Hammer 2012). The chemical weathering reactions of olivine involve a volume expansion that results in stress-induced fracture networks, increasing the permeability and porosity. In addition, hydration reactions are also highly exothermic so that local temperatures may exceed several tens of °C (Fyfe 1974; Kelemen and Hirth 2012).

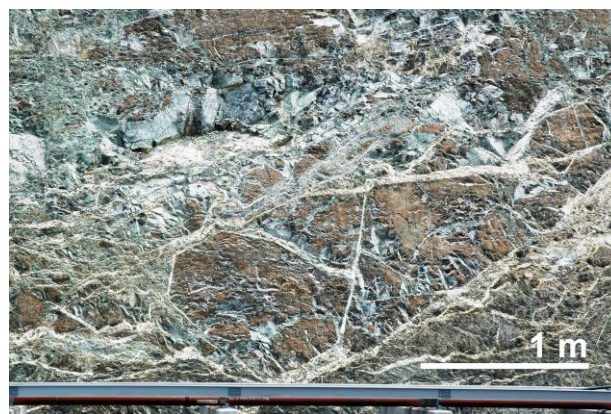


**Figure 1.** Field evidence of intense fracturing within the serpentine sole of Koniombo, NC, where magnesite is formed from meteoric fluids within fractures.

When combined together, the reaction-induced fracturing and reaction-induced heating may trigger thermal convection. In the case of ultramafic rocks, olivine hydration is highly exothermic ( $250 \text{ kJ kg}^{-1}$ ) and a rough estimate of the equivalent heat production rate (accounting for a weathering timescale of 40,000 years per meter) leads to values around 1 to  $10 \text{ W m}^{-3}$ .

In NC regolith, the intense fracturing (Figure 1) is characterized by present-day permeability values around  $5 \cdot 10^{-14} \text{ m}^2$  (for the fine yellow saprolite) to  $4.3 \cdot 10^{-13} \text{ m}^2$  in the coarse saprolite (Figure 2). These numerical values are used below to investigate whether physical conditions for the occurrence of thermal convection can be reached.

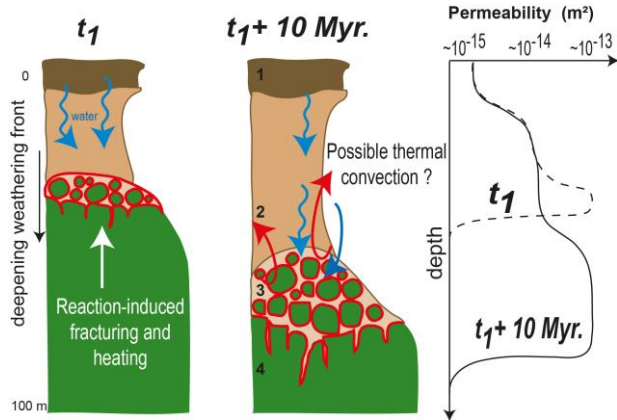


**Figure 2.** Simplified lateritic profile over ultramafic rocks of NC, showing two distinct depth levels of the weathering front. Four main layers are distinguished: 1: ferricrete; 2: red mottled zone and yellow fine saprolite; 3: coarse saprolite; 4: unweathered peridotites. On the left, thickness of the most permeable layer and temperature contrasts are not sufficient to trigger thermal convection. Ten Myr later, reaction-induced fracturing and heating (shown by red contours) may provide favorable conditions for thermal convection to occur. On the right: temporal evolution of depth-dependent permeability within the lateritic profile.

### 3 Corrugated bedrock topography

Figure 3a and 3b shows geological evidence of a corrugated bedrock topography. To date, undulations of the bedrock topography have been interpreted as due to variations in fracture density and/or in degree of serpentinization. However, it is proposed below that variations in fluid flow regime (occurrence of thermal convection) may also create the observed bedrock topography

At Tiébaghi, north-west of NC, Electric Resistivity Tomography (ERT) profiles (Beauvais et al. 2007) show undulated bedrock topography (Figure 3c). These undulations are regularly spaced when the surface topographic slope is small, while an irregular topography of the weathering front is depicted under a sloping surface. The temperature-dependence of resistivity is rarely invoked in studies based on geoelectrical methods. However, accounting for temperature dependence, fluid resistivity decreases linearly from  $\approx 100 \text{ } \Omega \text{ m}$  at  $0^\circ\text{C}$  to  $\approx 40 \text{ } \Omega \text{ m}$  at  $100^\circ\text{C}$ . Hence, the undulated topography of the weathering front could also correspond to the thermal imprint of previously warm fluids flowing within the laterite.

### 4 Likelihood of hydrothermal convection

In NC, permeability values in the saprolite layers are high, and anomalously high temperatures may occur at the level of the bedrock-saprolite interface if an

anomalously high temperature gradient is assumed, contrarily to the Quesnel et al. (2013) study. Such conditions may trigger efficient thermal convection, unless pressure-driven fluid flow dominates over buoyancy-driven flow.

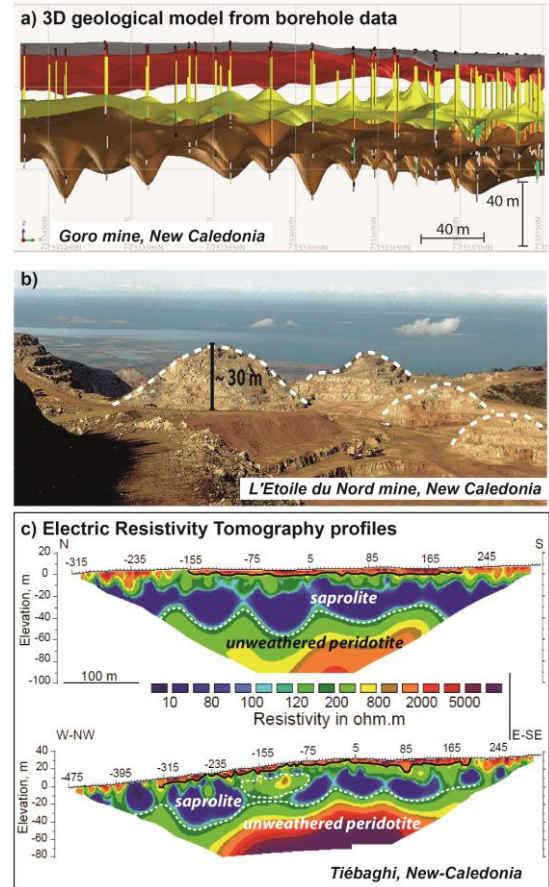


**Figure 3.** Topographic undulations of saprolite-bedrock interface; a) 3D model of geological interfaces of the Goro laterite (southern New Caledonia), as inferred from borehole data (vertical colored lines). The brown interface is the base of coarse saprolite (top of bedrock); b): large-scale and regularly spaced unweathered peridotite protrusions, Etoile du Nord Mine, north-west coast of New Caledonia; c) ERT profiles, Tiébaghi, New Caledonia, after Beauvais et al. (2007). The white dashed line delineates the weathering front.

For a flat topography and a constant-thickness aquifer, thermal convection in a porous medium can occur as soon as the Rayleigh number exceeds the critical value of  $4\pi^2$  (Lapwood 1948):

$$Ra = \frac{g \alpha \Delta T k H}{\kappa \nu} > 4\pi^2$$

where  $g$  is gravity,  $\alpha$  is the thermal expansion coefficient of water,  $\Delta T$  is the imposed temperature contrast,  $k$  is the medium permeability,  $H$  is the layer thickness,  $\kappa$  is the thermal diffusivity of water and  $\nu$  its kinematic viscosity. When typical water properties at  $20^\circ\text{C}$  are used for a 100m-thick aquifer in which a  $60^\circ\text{C}$  temperature contrast is present, then a permeability greater than  $\approx 3 \cdot 10^{-13} \text{ m}^2$  is needed to trigger convection.

In fact, when different conditions are considered, the critical Rayleigh number decreases to 3 (Phillips 1991), and convection can occur for a



permeability lower than  $10^{-13} \text{ m}^2$ . In addition, if the above physical properties are taken at  $50^\circ\text{C}$ , then thermal convection is triggered for even lower permeability values, around  $2 \times 10^{-14} \text{ m}^2$ .

The present-day permeability values for the coarse saprolite of New Caledonia have been estimated at  $4.3 \times 10^{-13}$ ; it is thus probable that values around  $10^{-12} \text{ m}^2$  were reached when fluid flow was more efficient. Consequently, although layers and interfaces are rarely flat, the physical conditions at which hydrothermal convection occurs are very likely to be reached. To proceed further in such investigations while accounting for realistic properties and representative geometries of the weathering layers, a numerical approach is required.

## 5 Numerical modeling

Thermal convection within permeable media can be numerically studied by coupling heat transfer and fluid flow equations with the appropriate fluid and rock physical properties. Using Comsol Multiphysics™ software (finite element method), Darcy law and heat equation in porous media have been coupled with temperature-dependent fluid density and viscosity.

Model set-up and boundary conditions are illustrated in Figure 4. Preliminary models consider a constant permeability medium. The second series of experiments include the weathering front deepening, by simulating an increase in heat production and permeability at the front level.

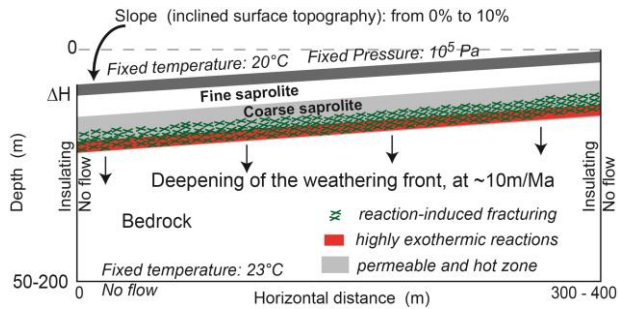


**Figure 4.** Model set-up and boundary conditions for the case of deepening weathering front, which is characterized by a permeability increase and a high heat production rate.

### 5.1 Preliminary models (constant permeability)

Preliminary models of hydrothermal convection were performed in order to retrieve the velocity estimates of  $0.4$  to  $1.5 \times 10^{-7} \text{ m.s}^{-1}$ , given by Join et al. (2005). A fixed temperature condition of  $80^\circ\text{C}$  is imposed at the base of the medium, whose surface topography varies from 1 to 10%; a constant permeability value  $k_{lat}$  ( $10^{-15}$  to  $10^{-12} \text{ m}^2$ ) is imposed to the medium. The lower velocity estimate is reached for slopes greater than  $\sim 7\%$ , implying permeability greater than  $\sim 8 \times 10^{-14} \text{ m}^2$ , and involving weak convection. However, the highest velocity estimate of  $1.5 \times 10^{-7} \text{ m.s}^{-1}$  can be reached only when thermal convection is fully developed, regardless of the slope.

The critical permeability values for which transition from topography-driven to buoyancy-driven fluid flow occurs, depend on the layer thickness and topographic slope (Figure 5). The bottom-left part of the diagram corresponds to conditions for which topography

and gravity control fluid flow.

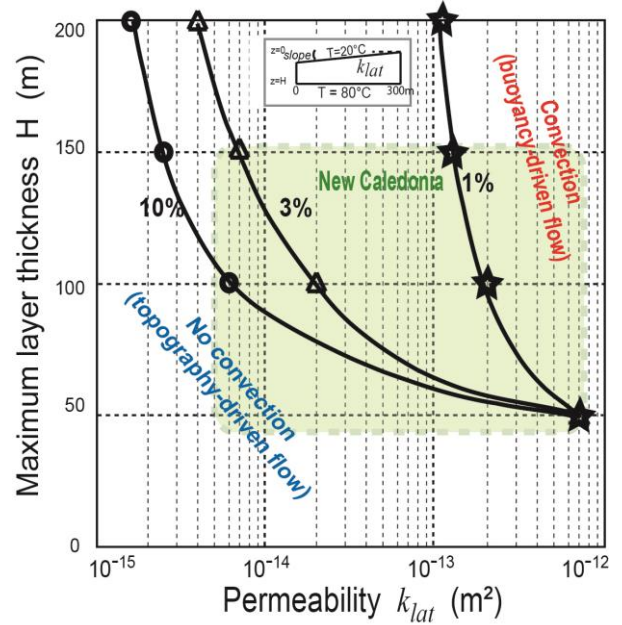


**Figure 5.** Constant permeability models. For a 100 m – thick laterite with a permeability of  $2 \times 10^{-14} \text{ m}^2$  (triangle symbol) hydrothermal convection can occur as soon as the topographic slope is lower than 3%.

The top-right part includes conditions for a regime of buoyancy-driven fluid flow. Although these constant permeability models are simplified compared to natural lateritic profiles, the location of the green area representing the  $H$  and  $k_{lat}$  domains in the laterites of New Caledonia, implies that the occurrence of hydrothermal convection is as much probable as fluid flow regimes driven only by gravity and topography.

### 5.2 Models with a deepening weathering front

Exothermic reactions can be simulated at the weathering front by an equivalent heat production value such that high temperatures (several tens of  $^\circ\text{C}$ ) can be obtained after several million years of weathering, deepening to a few tens of meters.

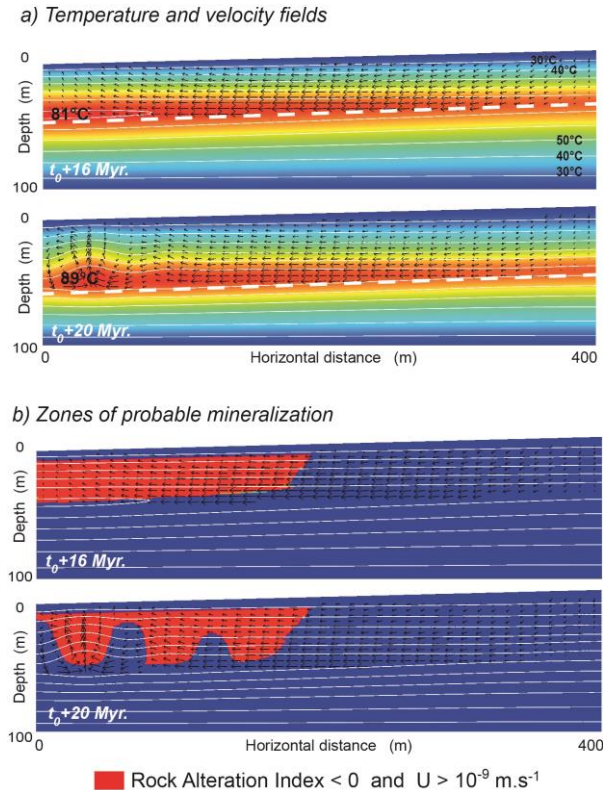
The vertical extent of exothermic reactions was simulated by using a semi-Gaussian type function, whose half-width can be adjusted. This thermal thickness was typically 5 to 10 meters high. A similar time- and depth-dependent function was also used for the permeability, but with a thicker extent.

Figure 6a illustrates an experiment where hydrothermal convection is triggered 16 Myr after the beginning of the experiment. At that time, temperature contrast (around  $60^\circ\text{C}$ ) through the thick (60 m) permeable layer (up to  $7 \times 10^{-13} \text{ m}^2$ ) permits convection. Hydrothermal convection results in the uplifting of the isotherms, related to upward fluid motion.

Figure 6b illustrates, for the same experiments, the zones where the Rock Alteration Index (Philips 1991) is large and negative. Expressed as the scalar product of the fluid velocity by the temperature gradient, the RAI corresponds to a local cooling rate. In other words, the red zones delineate the areas where the local cooling rates are the highest, and where fluid velocity is larger than a given threshold value of  $10^{-9} \text{ m.s}^{-1}$ . Hence,

the red zones correspond to the most weathered and mineralized areas, while the blue zones show the less weathered areas. For the same physical properties as in Figure 6a, but with a 7.5% slope, corrugations do not develop because the fluid velocity component due to topography-driven flow dominates.

Figure 7 shows the transient evolution of the RAI pattern over a few Myrs, for a faster front velocity and for two different slopes.



**Figure 6.** Results for an experiment where the weathering front deepens at a velocity of  $2.5 \text{ m Myr}^{-1}$ . Maximum equivalent heat production and permeability are  $0.8 \text{ W m}^{-3}$  and  $7 \cdot 10^{-13} \text{ m}^2$ . a) temperature (colour and black contours) and velocity field (arrows); b) Red zones show areas of intense weathering, where mineralization is probable. In the blue zones, the weathering is no longer efficient.

## 6 Conclusion

Although we did not model a natural topographic profile that would include plateaus and/or slope changes, any attempt to reproduce field observations in greater detail should also account for additional effects, e.g. chemical and mechanical erosion, tectonic and climatic forcings, as well as meteoric water influence.

The influence of exothermic reactions on groundwater circulations is still poorly known, but our results suggest that convective flow might have developed in weathered ultramafic rocks of New Caledonia.

## Acknowledgements

This study was funded by BRGM Research Division, through the “S-Chaud/313” research project.

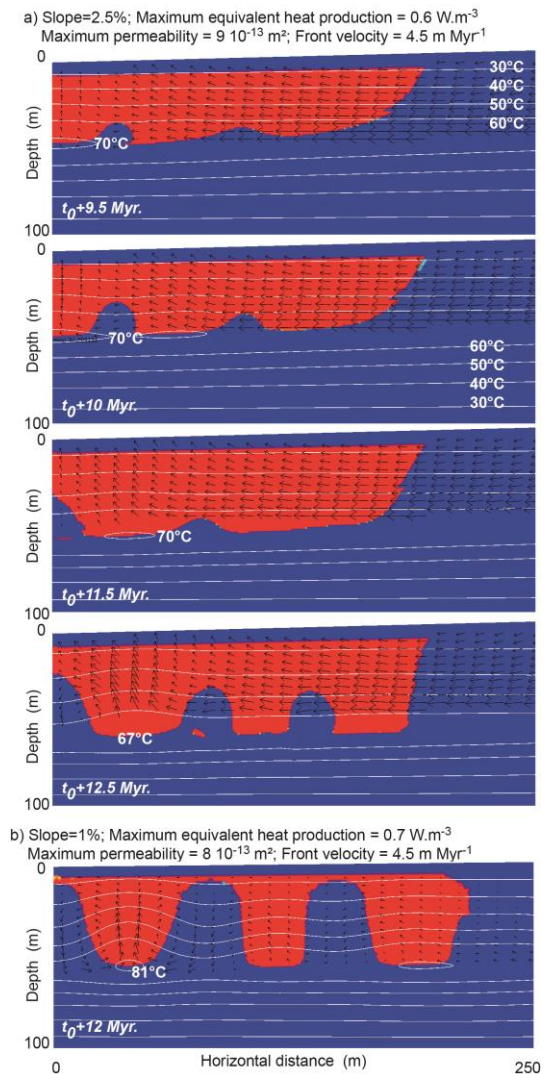


**Figure 7.** Transient evolution for the case of a high permeability, with two different slopes: a) 2.5% and b) 1%.

## References

- Beauvais A, Parisot JC, Savin C (2007) Ultramafic rock weathering and slope erosion processes in a South West Pacific tropical environment. *Geomorphology*, 83, 1-13
- Fyfe WS (1974) Heats of chemical reactions and submarine heat production. *Geophys. J. Roy. Astr. Soc.*, 37, 213-215
- Jamtveit B, Hammer O (2012) Sculpting of rocks by reactive fluids. *Geochem. Persp.*, 1, 3, 341-480
- Join JL, Robineau B, Ambrosi JP, Costis C, Colin F (2005) Système hydrogéologique d'un massif minier ultrabasique de Nouvelle-Calédonie. *C. R. Geosc.*, 1500-1508
- Kelemen PB, Hirth G (2012) Reaction-driven cracking during retrograde metamorphism: olivine hydration and carbonation. *Earth Planet. Sci. Lett.*, 345-348, 81-89
- Lapwood E (1948) Convection of a fluid on a porous medium. *Proc. Camb. Phil. Soc.*, 44, 508-521
- Phillips O (1991) Flow and reactions in permeable rocks, Cambridge University Press, New York
- Quesnel B, Gautier P, Boulvais P, Cathelineau M, Maurizot P, Cluzel D, Ulrich M, Guillot S, Lesimple S, Couteau C (2013) Syn-tectonic, meteoric water-derived carbonation of the New Caledonia peridotite nappe. *Geology*, 41, 1063-1066
- Trescases J.J. (1975). L'évolution géochimique supergène des roches ultrabasiques en zone tropicale. Formation des gisements nickélicifères de Nouvelle-Calédonie. *Mémoires de l'ORSTOM*, 78, Paris, pp. 259